

ICPES 2025

40th INTERNATIONAL CONFERENCE ON PRODUCTION ENGINEERING - SERBIA 2025

DOI: 10.46793/ICPES25.397M



University of Nis
Faculty of Mechanical
Engineering

Nis, Serbia, 18 - 19th September 2025

EXPERIMENTAL EVALUATION OF TENSILE PROPERTIES OF 3D-PRINTED PLA THREADS

Miroslav MIJAJLOVIĆ^{1*}, Gordana JOVIĆ², Aleksandar TRAJKOVIĆ¹, Miloš MADIĆ¹, Jovan ARANĐELOVIĆ¹, Nikola KORUNOVIĆ¹

Orcid: 0000-0001-9185-8296; Orcid: 0009-0006-1390-8167; Orcid: 0000-0002-2310-2590;
Orcid: 0000-0001-9653-4119; Orcid: 0000-0002-9103-9300;

¹University of Niš, Faculty of Mechanical Engineering in Niš, Niš, Serbia

²The Academy of Applied Technical and Preschool Studies, Niš, Serbia

*Corresponding author: miroslav.mijajlovic@masfak.ni.ac.rs

Abstract: This study presents an experimental investigation into the tensile behavior of threads and specimens fabricated using polylactic acid (PLA) filament via fused deposition modeling (FDM). While tensile properties of bulk PLA samples and structural components have been widely explored, the mechanical performance of isolated, stand-alone printed threads remains underreported. Such analysis is vital given that the integrity of thin structural surfaces is heavily dependent on the strength and stability of their embedded threads. To investigate this topic, PLA threads were printed using controlled parameters and subjected to standardized tensile testing. Key mechanical properties, including ultimate tensile strength, elongation at break, number of threads and Young's modulus, were determined, compared and discussed. These results provide a foundation for optimizing printing procedures and techniques towards adaptive printing.

Keywords: Tensile Properties, PLA, Threads.

1. INTRODUCTION

Tensile testing represents a fundamental and well-established technique for characterizing the mechanical properties of engineering materials and structural elements. The tensile-derived parameters, such as yield strength, ultimate tensile strength, elastic modulus, and strain, serve as a reliable foundation for extrapolating other material behaviors and for optimizing structural performance within specific geometrical and loading contexts. Tensile characterization of polylactic acid (PLA), a widely utilized biodegradable thermoplastic additive

manufacturing, is typically conducted in accordance with standardized protocols such as ASTM D638 [1] and ISO 527-1 [2]. Specimens are fabricated via fused deposition modeling (FDM) and subsequently subjected to uniaxial tensile loading until mechanical failure. This methodology enables the quantification of critical parameters, including ultimate tensile strength, elastic modulus, and elongation at break [3, 4]. The resulting mechanical behavior is highly dependent on process variables such as layer height, raster orientation, and infill density, which affect interlayer adhesion and internal microstructure. Tensile testing serves

as a foundational tool for optimizing printing conditions in structural/functional applications.

In recent studies, the tensile behavior of PLA has been extensively investigated under differing conditions. Poddar and Sarangi assessed how extrusion parameters influence the tensile strength of PLA filaments, applying Taguchi and ANOVA methodologies to quantify effects of temperature [5]. Complementarily, Domerg et al. examined the impact of ambient aging and specimen geometry on 3D-printed PLA, demonstrating notable variations in ductility and fracture response due morphological and temporal factors Stojković and Turudija review how fiber type and thread overall, alignment, and printing conditions critically affect the tensile and structural performance of carbon fiber reinforced PLA composites fabricated via FFF [7]. Alparslan et al. demonstrated that PLA specimens printed via FDM with a 0.15 mm layer thickness and hexagonal infill showed optimal tensile strength, while increased layer height led to reduced strength and ductility [8].

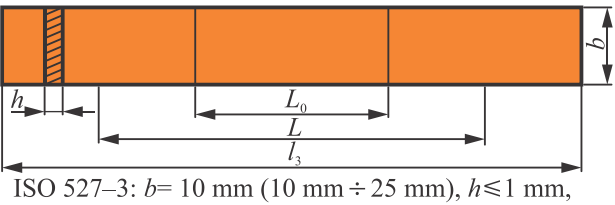
2. SPECIMEN DESIGN, FABRICATION AND TESTING PROCEDURE

Tensile testing of PLA printed parts is performed according to standardized protocols to ensure accurate evaluation of mechanical properties. Specimens are designed and fabricated via FDM with controlled parameters, then conditioned under ambient conditions prior to mechanical testing. Using a universal testing machine, uniaxial load is applied on test specimens until fracture, while force and elongation data are captured to derive stressstrain behavior. Key metrics, such as tensile strength, modulus, and elongation, determined, and post-fracture analysis reveal failure modes.

2.1 Determination of tensile properties

The general methodology for evaluating tensile properties is described in ISO 527-1. Specific testing conditions applicable to thin plastic films, defined as materials with a thickness $h \le 1$ mm, are provided in ISO 527-3

[10]. Testing specimens should be strips (type 2), dimensioned as given in Figure 1.



ISO 527–3: $b = 10 \text{ mm} (10 \text{ mm} \div 25 \text{ mm}), h \le 1 \text{ mm}, L_0 = 50 \text{ mm} \pm 0.5 \text{ mm}, L = 100 \text{ mm} \pm 5 \text{ mm}, l_3 \le 150 \text{ mm}$

Figure 1. ISO 527-3: Test specimen, shape and dimensions

According to the ISO 527-3, test specimens shall be fabricated either through additive manufacturing or as cutouts, ensuring they remain unpolished, unbonded, and free from macroscopic defects. Each testing protocol shall be conducted on a minimum of five geometrically and materially identical specimens, conforming to the standards and specifications outlined in ISO 527-1.

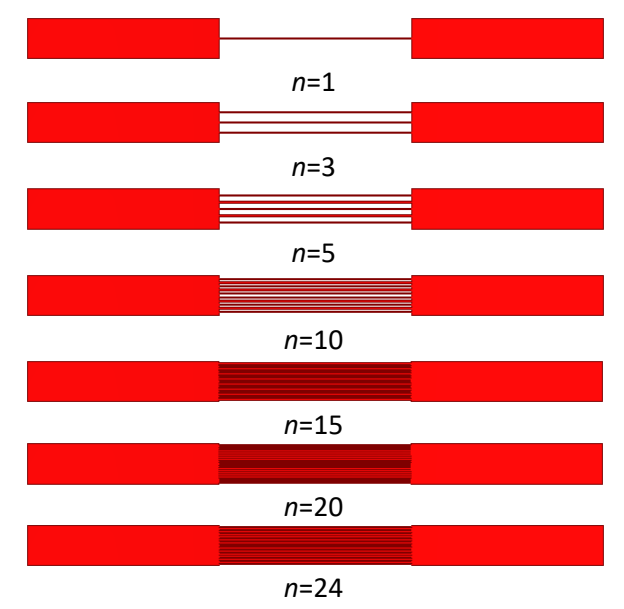


Figure 2. Virtual (CAD) specimens

2.1 CAD model of specimens

Virtual specimens (CAD models) were designed using Autodesk Inventor Academic, modeled as three-dimensional components with geometric parameters corresponding to those illustrated in Figure 1.

To investigate the load-bearing behavior of individual and grouped extruded threads (representing 3D printed lines), the central gauge section of each specimen (L_0) was systematically varied. This region was modeled to incorporate 1, 3, 5, 10, 15, 20, and 24 parallel threads, resulting in the generation of seven distinct specimen types (Figure 2).

2.2 3D printing

All 7 types of the testing specimens (35 specimens in total) are created/printed using the Creality Ender 3 V3 SE 3D printer (Figure 3).



Figure 3. Creality Ender 3 **Figure 4.** Filament type V3 SE 3D printer

The slicing of CAD models was performed using Ultimaker Cura 5.6.0. The printing process was conducted with the 0.4 mm diameter nozzle, at a nozzle temperature of 225 °C and a heated bed temperature of 70°C. The layer height was set to 0.2 mm, and the total height of each specimen corresponded to a single printed layer.

The printing speed was precisely defined for different parts of the model: outer wall, inner wall, and general wall speeds were all set to 90 mm/s, while the initial layer was printed at a reduced speed of 15 mm/s to improve adhesion to the build plate. The overall print speed was set to 180 mm/s. A 100% infill density with a lines infill pattern was used to ensure complete volumetric solidity of the specimens. No support structures were applied, nor were any build plate adhesion methods (skirt, brim, or raft) used. Prior to printing, automatic mesh bed levelling was enabled to ensure consistent layer height across the build surface.

Printing has been performed in two stages:

- 1. In the initial stage, the threads were printed in a single, uninterrupted pass to ensure continuity and structural integrity. Each thread measured l_3 =150 mm in length, with a layer height of h=0.2 mm and a line width of b_1 =0.4 mm.
- 2. During the second stage, the specimen's gripping regions were printed at full scale on both ends, each with a printed length of l=50 mm, a pass height of h=0.4 mm, and thread width $b_1=0.4$ mm. This additional layer thermally fused with the previously deposited filaments through material overlap, thereby securing their position within the sample geometry. Notably, the central threads, spanning the full length, remained virtually intact and unaffected by the secondary printing operation.

As a fillament material, HP Ultra – PLA is used (Figure 4). HP Ultra – PLA filament is degradable PLA (Polylactic Acid), material codeveloped by Creality and BASF as a high-quality, reliable material known for its ease of printing, stable performance, giving high quality of the printed parts. The manufacturers report that HP Ultra PLA has Young's elasticity modulus of $E=2970-3050 \, \text{MPa}$ (in plane), ultimate strength of maximal $R_m=75 \, \text{MPa}$ and ultimate strain (strain at ultimate strength) $\epsilon_m=3 \,\%$ [9].

2.3 Testing machine

The tensile testing procedure shall be conducted using a machine conforming to the requirements outlined in ISO 7500-1 [11] (verification of static uniaxial testing machines) and ISO 9513 [12]. Testing speeds shall be set at one of the following discrete values: v=5/50/100/200/300/500 mm/min, based on the material behavior and experimental protocol (in this case v=10 mm/min).

Quasi-static uniaxial tensile tests were carried out with a Shimadzu Table-top AGS-X 10 kN universal testing machine (UTM), which is shown in Figure 5. This UTM is comprised of a rigid frame (stroke distance 1200 mm), crosshead (speed range 0.001-1000 mm/min, with an accuracy of 0.1%), test grips (for holding the specimen), force sensors (load cell with a maximum of 10 kN), and a control unit (up to 1 kHz accuracy).



Figure 5. Shimadzu Table-top AGS-X UTM

With the mentioned characteristics this UTM ensures the uniform transfer of force to the test specimen which is fixed with the grips and subjected to pulling (tensile) forces in the axial direction until it breaks. During this process force-stroke points are recorded with the Shimadzu TrapeziumX software with a 100 Hz frequency, based on which the software can produce a force-stroke curve for each tested specimen.

2.4 Data acquisition

Dimensional accuracy at the initial gauge length (L_0 =0 mm) is assumed to be within a tolerance of 1%. The data acquisition rate shall be maintained at f=100 Hz, ensuring adequate resolution for both force and strain measurements according to applicable metrological standards.

The use of dumb-bell shaped specimens that exhibit breakage or slippage within the gripping zones is strictly prohibited. A prestrain of $\epsilon_0 \le 0.05\%$ shall be applied to all test specimens prior to initiating the tensile test, in order to stabilize the material response and minimize initial slack.

The standardized report for each test shall be labeled in accordance with ISO nomenclature as ISO 527-3/2/50, reflecting the specimen type, test conditions, and measurement parameters.

2.5 Estimation of tension stress, strain and modulus

Since nominal cross section A_n of the fully printed test specimen shall be:

$$A_n = b \cdot h = 10 \cdot 0.2 = 20 \,\text{mm}^2$$
, (1)

the maximal cross sections of the printed sample sets are 4%, 12%, 20%, 40%, 60%, 80% and 96% of A_n , for n=1, 3, 5, 10, 15, 20 and 24 threads. Since the number of unbroken threads n(t) changes during testing $(n(t) \le n)$, the true cross section of the testing sample is:

$$A_{n(t)} = n(t) \cdot b_1 \cdot h. \tag{2}$$

Finally, the engineering stress σ_e [MPa] in the samples is estimated as:

$$\sigma_e = \sigma_{n(t)} = F/A_{n(t)}, \tag{3}$$

where F [N] is the measured tension force.

The engineering strain ε_e [-] is estimated as:

$$\varepsilon_e = \Delta L_0 / L_0, \tag{4}$$

where: L_0 [mm] is the gauge length of the test specimen, ΔL_0 [mm] is the increase of the specimen length between the gauge marks.

The tensile modulus E [MPa] is estimated using linear regression procedure applied on the stress/strain curve in the strain interval $0.0005 \le \epsilon \le 0.0025$, using the expression:

$$E = d\sigma_e / d\varepsilon_e, (5)$$

where $d\sigma_e/d\varepsilon_e$ is the slope of a least-squares regression line fit to the part of the stress/strain curve.

The true stress σ and true strain ϵ are estimated as:

$$\sigma = \sigma_e (1 + \varepsilon_e) \tag{6}$$

$$\varepsilon = \ln(1 + \varepsilon_e) \tag{7}$$

True stress/ strain are used for accurate definition of both elastic and plastic behaviour of materials by considering the actual cross section of the test specimens.

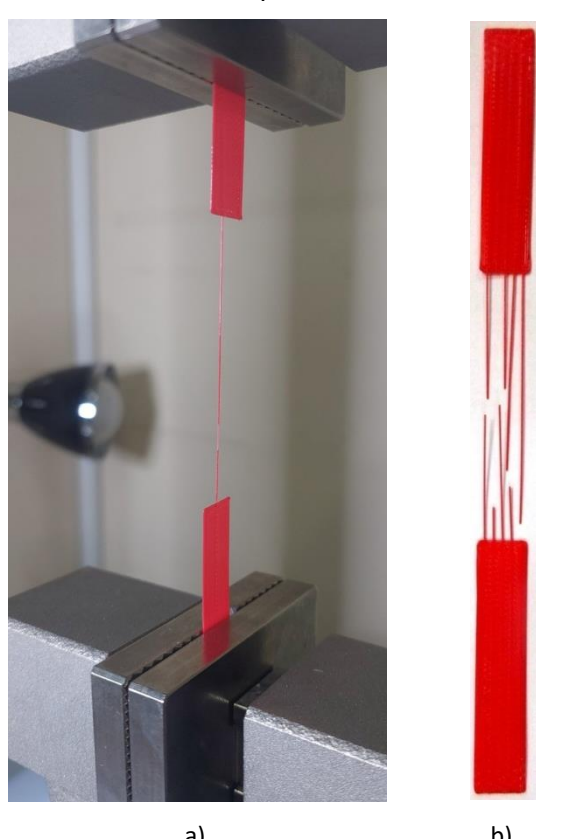


Figure 6. Experimental testing: a) test specimen in testing machine, b) broken test specimen

3. RESULTS AND DISCUSSION

All specimens underwent experimental testing under standardized conditions. The same testing protocols, procedures, and measuring equipment were used throughout, ensuring consistency of the results (Figure 6).

All of the samples with n=1 threads exhibit typical stress-strain curve diagrams (Figure 7).

exhibited stress-strain specimens behavior characteristic of tensile failure, wherein the applied stress reached the expected peak tensile strength prior to specimen fracture. This indicates that failure occurred post-maximum stress, confirming that the structural integrity of the samples was maintained up to the point of ultimate loadbearing capacity.

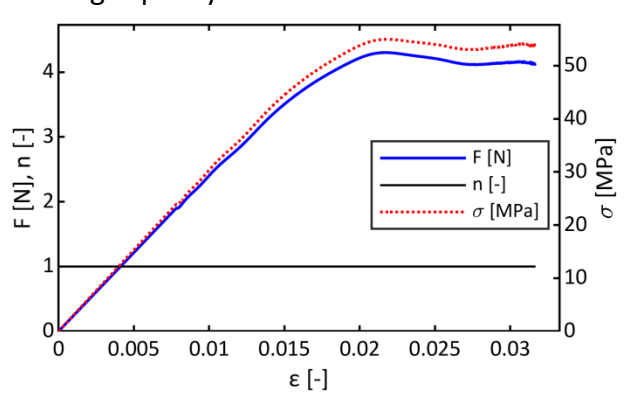


Figure 7. Tension force, number of unbroken treads, and true stress vs. true strain (n1/#1)

The specimen number (#), maximal tension force in the specimen (F_{max}), maximal tension force in the thread(s) ($F_{max'}$), stress at 0.2% strain (R_{p02}) , strength (R_m) , modulus (E), strain of 0.2% (ε_{p02}), strain at R_m (ε_m), median value (M), and standard deviation (SD) are shown in Table 1. The same nomenclature is used for all testing specimens.

Table 1. Test specimens #1-#5 with n=1 – results

#	F _{ma}	F _{max} '	R_{p02}	R_m	Ε	<i>E</i> _{p02}	€m
	Х						
[-	[N]	[N/t	[MP	[MP	[MP	[-]	[-]
]		hr]	a]	a]	a]		
1	4.3	4.35	53.2	55.6	2891	0.0	0.0
	55	5	50	60		20	22
2	4.9	4.98	61.7	63.1	3063	0.0	0.0
	81	1	79	37		22	24

3	4.9	4.97	58.7	62.9	3166	0.0	0.0
	70	0	08	94		21	25
4	4.8	4.86	57.0	61.6	3267	0.0	0.0
	64	4	32	28		19	23
5	4.3	4.35	53.0	54.9	3035	0.0	0.0
	55	5	45	62		19	22
М	4.7	4.70	56.7	59.6	3084	0.0	0.0
:	05	5	63	76		20	23
S	0.3	0.32	3.71	4.03	141.	0.0	0.0
D	23	3	4	6	689	01	01
:							

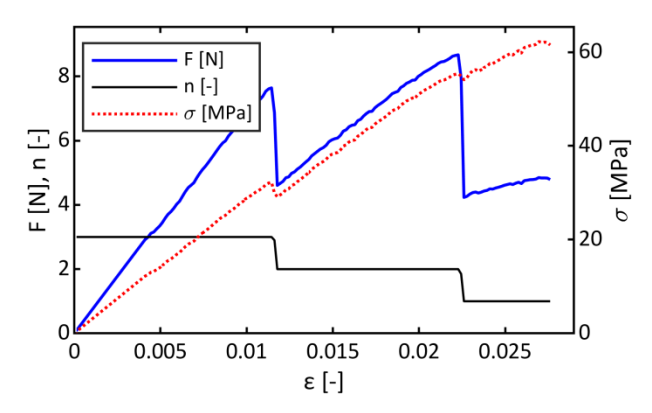


Figure 8. Tension force, number of unbroken treads, and true stress vs. true strain (n3/#3)

Test samples with n=3 threads exhibit typical stress-strain curve diagrams (Figures 8 and 9). Thread rupture occurred at random locations across specimens, indicating non-uniform failure initiation.

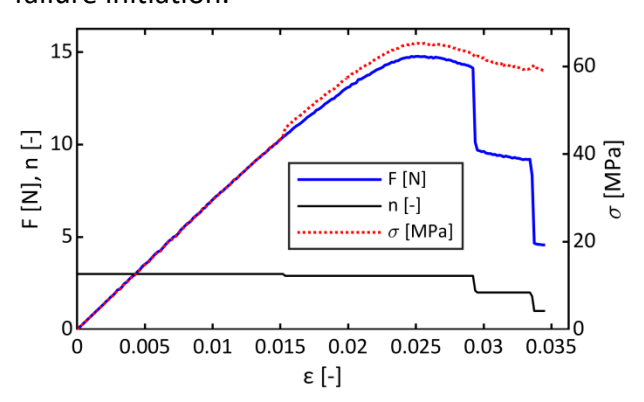


Figure 9. Tension force, number of unbroken treads, and true stress vs. true strain (n3/#4)

Test specimens n3/#1, n3/#2, n3/#3, and n3/#5 exhibit rupture and breakage of at least one thread before reaching the strength of the specimen. The specimen n3/#3 shows rupture of threads before reaching the maximal strength of the specimen; destruction of the treads appears afterwards, one thread after

another. The summarized results are shown in the Table 2.

Table 2. Test specimens #1-#5 with n=3 – results

#	F_{max}	$F_{max'}$	R_{p02}	R_m	Ε	<i>E</i> p02	\mathcal{E}_m
[-	[N]	[N/t	[MP	[MP	[MP	[-]	[-]
]		hr]	a]	a]	a]		
1	10.3	5.03	59.7	63.4	300	0.0	0.0
	03	1	03	45	5	22	26
2	10.5	4.96	63.2	63.3	291	0.0	0.0
	16	3	95	75	2	24	24
3	8.68	4.84	47.3	62.3	296	0.0	0.0
	5	9	18	11	8	18	27
4	14.7	5.09	64.0	65.2	294	0.0	0.0
	74	3	75	89	3	24	25
5	12.0	4.90	61.9	62.8	298	0.0	0.0
	37	2	80	19	2	23	25
М	11.2	4.96	59.2	63.4	296	0.0	0.0
:	63	8	74	48	2	22	26
S	2.29	0.09	6.88	1.12	35.8	0.0	0.0
D	4	8	6	7	68	02	01
:							

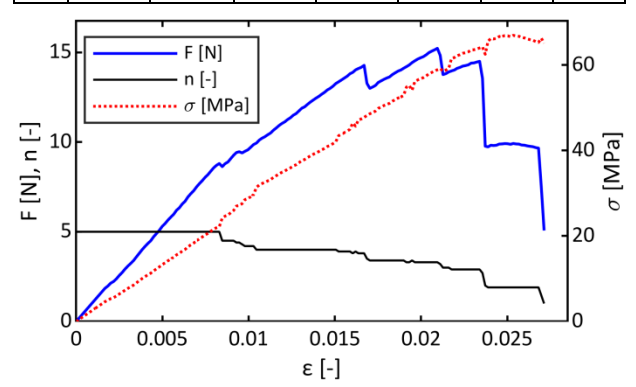


Figure 10. Tension force, number of unbroken treads, and true stress vs. true strain (n5/#4)

All test samples with *n*=5 threads exhibit rupture and breakage of the threads before reaching the strength of the specimen (Figure 10).

The strength of the specimens is comparable to the strength of the previously tested specimens. It is reached in all specimens (having $n(t) \ge 2$ treads unbroken at the moment of reaching strength). The summarized results are shown in the Table 3.

Table 3. Test specimens #1-#5 with n=5 – results

#	F _{max}	F _{max} '	R_{p02}	R _m	Ε	\mathcal{E}_{p02}	\mathcal{E}_m
[-	[N]	[N/t	[MP	[MP	[MP	[-]	[-]
]		hr]	a]	a]	a]		
1	18.	4.90	60.	62.	2712	0.0	0.0
	636	6	368	975		24	26
2	23.	4.95	56.	63.	2835	0.0	0.0
	648	1	474	452		22	25
3	19.	4.91	52.	63.	2501	0.0	0.0
	827	3	983	554		23	34
4	15.	5.22	66.	66.	2749	0.0	0.0
	246	2	184	948		26	25
5	19.	5.10	63.	65.	2810	0.0	0.0
	259	4	493	445		25	25
М	19.	5.01	59.	64.	2721	0.0	0.0
:	323	9	900	475		24	27
S	3.0	0.13	5.2	1.6	132.	0.0	0.0
D	02	9	96	73	459	02	04
:							

All test samples with n=10 threads also exhibit rupture and breakage some of the threads before reaching the strength of the sample (Figure 11).

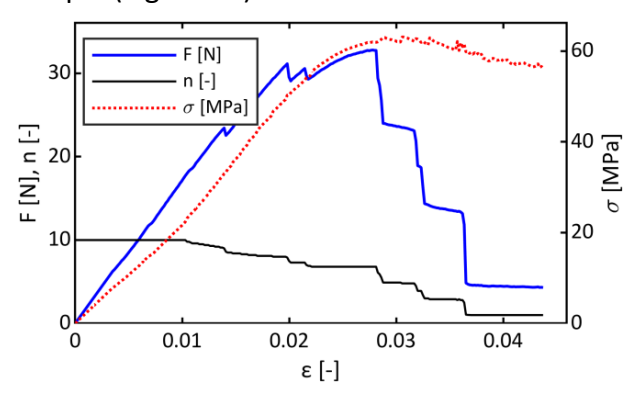


Figure 11. Tension force, number of unbroken treads, and true stress vs. true strain (n10/#2)

The strength of the specimens is comparable to the strength of the previously tested specimens. It is reached in all specimens (having $n(t) \ge 5$ unbroken treads at the moment of reaching strength). The summarized results are shown in the Table 4.

All test specimens with n=15 threads also exhibit rupture and breakage some of the threads before reaching the strength of the sample (Figures 12).

Table 4. Test specimens #1-#5 with n=10 – results

#	F _{max}	F _{max} '	R _{p02}	R _m	Ε	<i>E</i> _{p02}	\mathcal{E}_m
[-	[N]	[N/t	[MP	[MP	[MP	[-]	[-]
]		hr]	a]	a]	a]		
1	43.	5.05	62.	65.	2548	0.0	0.0
	538	2	433	098		27	30
2	32.	4.89	62.	63.	2103	0.0	0.0
	808	6	229	092		32	31
3	30.	5.26	61.	66.	2042	0.0	0.0
	573	7	698	713		32	28
4	34.	5.12	65.	65.	2543	0.0	0.0
	626	4	127	929		28	29
5	42.	4.85	59.	62.	2531	0.0	0.0
	934	1	984	357		26	28
М	36.	5.03	62.	64.	2353	0.0	0.0
:	896	8	294	638	.4	29	29
S	5.9	0.16	1.8	1.8	257.	0.0	0.0
D	67	9	53	56	405	03	01
:							

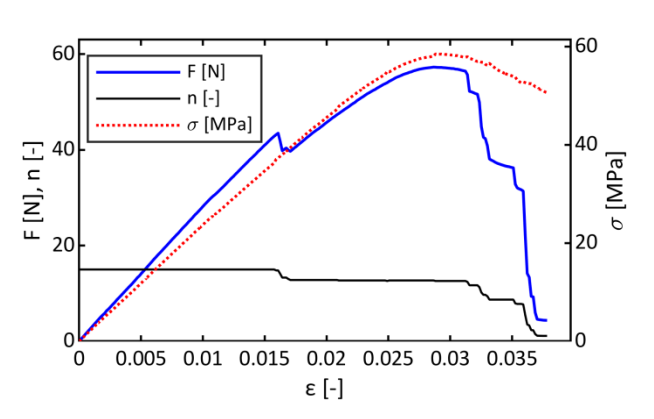


Figure 12. Tension force, number of unbroken treads, and true stress vs. true strain (n15/#1)

The strength of the specimens is comparable to the strength of the previously tested specimens. It is reached in all specimens (having $n(t) \ge 7$ unbroken threads at the moment of reaching strength). The summarized results are shown in the Table 5.

Table 5. Test specimens #1-#5 with n=15 – results

#	F _{max}	F _{max} '	R_{p02}	R _m	Ε	\mathcal{E}_{p02}	\mathcal{E}_m
[-	[N]	[N/t	[MP	[MP	[MP	[-]	[-]
]		hr]	a]	a]	a]		
1	57.2	4.54	54.1	58.4	237	0.0	0.0
	98	5	35	71	2	25	29
2	54.4	5.09	64.4	65.4	233	0.0	0.0
	33	2	56	81	1	30	28
3	52.2	4.90	62.1	63.1	242	0.0	0.0
	84	3	67	13	1	28	29

4	49.0	4.70	57.0	60.5	238	0.0	0.0
	46	6	70	01	9	26	28
5	48.2	5.07	61.0	65.3	238	0.0	0.0
	50	0	26	73	1	28	32
М	52.2	4.86	59.7	62.5	237	0.0	0.0
:	62	3	71	88	8	27	29
S	3.75	0.23	4.13	3.07	32.4	0.0	0.0
D	9	6	3	0	84	02	02
:							

All test samples containing n=20 threads showed signs of rupture, with several threads breaking prior to the sample reaching its full tensile strength (Figure 13).

The specimens demonstrated strength levels comparable to those observed in previously tested samples. In every case, the maximum strength was achieved with approximately $n(t) \ge 10$ threads remaining unbroken at the point of peak load. The summarized results are shown in the Table 6.

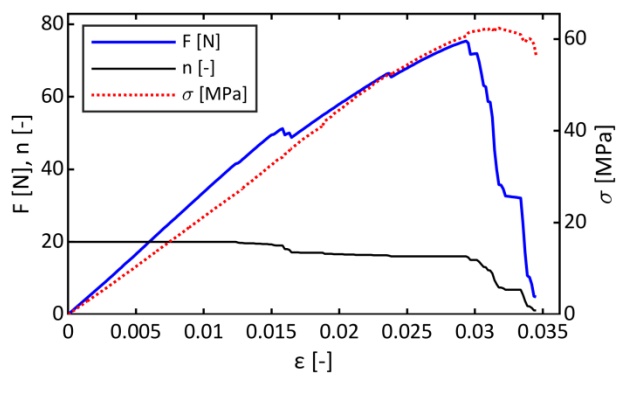


Figure 13. Tension force, number of unbroken treads, and true stress vs. true strain (n20/#5)

Table 6. Test specimens #1-#5 with n=20 – results

#	F _{max}	$F_{max'}$	R_{p02}	R _m	Ε	Е _{р02}	\mathcal{E}_m
[-	[N]	[N/t	[MP	[MP	[MP	[-]	[-]
]		hr]	a]	a]	a]		
1	70.	5.03	64.	64.	2217	0.0	0.0
	518	6	971	970		31	32
2	84.	4.77	56.	61.	2128	0.0	0.0
	162	1	191	475		28	34
3	67.	5.09	61.	65.	1947	0.0	0.0
	698	0	007	693		33	32
4	59.	4.86	60.	62.	2150	0.0	0.0
	579	6	320	620		30	29
5	75.	4.83	62.	62.	2156	0.0	0.0
	458	6	256	407		31	32
М	71.	4.92	60.	63.	2119	0.0	0.0
:	483	0	949	433		31	32

S	9.1	0.13	3.1	1.8	101.	0.0	0.0
D	31	6	99	04	977	02	02
:							

All test samples with n=24 threads also exhibit rupture and breakage some of the threads before reaching the strength of the sample (Figures 14).

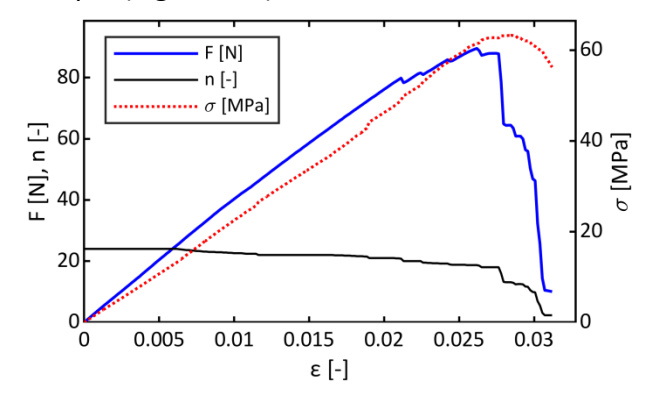


Figure 14. Tension force, number of unbroken treads, and true stress vs. true strain (n24/#2)

The tensile strength achieved in all specimens is consistent with that observed in previously tested samples. At the point of peak tensile load, each specimen retained at least $n(t) \ge 12$ unbroken threads, confirming uniform structural integrity across the test set. A summary of the results is presented in Table 7.

Table 7. Test specimens #1-#5 with n=24 – results

#	F _{max}	F _{max} '	R_{p02}	R _m	Ε	\mathcal{E}_{p02}	\mathcal{E}_m
[-	[N]	[N/t	[MP	[MP	[MP	[-]	[-]
]		hr]	a]	a]	a]		
1	70.5	5.03	62.	64.	198	0.0	0.0
	18	6	832	907	5	32	31
2	89.6	4.91	60.	63.	213	0.0	0.0
	95	9	444	257	5	30	28
3	100.	4.99	63.	64.	214	0.0	0.0
	315	6	657	444	4	32	31
4	94.3	4.94	63.	63.	209	0.0	0.0
	87	1	129	869	5	32	34
5	110.	4.61	56.	59.	212	0.0	0.0
	739	5	816	504	8	29	31
М	93.1	4.90	61.	63.	209	0.0	0.0
:	31	1	376	196	7	31	31
S	14.8	0.16	2.8	2.1	65.	0.0	0.0
D	86	6	31	55	500	01	02
:							

The maximum force per thread (F_{max}) is lowest for specimens with n=1 thread (4.705 N) and highest for those with n=10 threads (5.038 N). While the lower value at n=1 is expected, the elevated force observed at n=10 may be attributed to the greater number of unbroken threads present at the point of peak tensile strength.

The elastic modulus (*E*) exhibits a decreasing trend, with the highest value recorded in specimens containing a single thread (3084 MPa), and the lowest in specimens with 24 threads (2097 MPa). A slight deviation from this trend is observed at *n*=10 threads (2353 MPa), likely attributed to the increased number of unbroken threads.

The ultimate tensile strength (R_m) was lowest in single-threaded specimens (59.676 MPa) and highest in specimens with ten thread lines (64.638 MPa). Similarly, the 0.2% proof stress (R_{p02}) ranged from 56.763 MPa at n=1 to a maximum of 62.294 MPa at n=10. These increases are again attributable to the higher number of unbroken threads contributing to load-bearing during testing.

The 0.2% strain (ε_{p02}) was lowest in single-threaded specimens (0.020) and highest in specimens with 24 threads (0.031). A similar trend was observed for the strain at maximum tensile strength (ε_m), ranging from ε_m =0.020 at n=1 to a peak of ε_m =0.032 at n=20.

To define tensile properties of the samples, upon completing the full testing sequence for all 35 specimens, the data were aggregated, analyzed, normalized, and statistically refined (Table 8). Given the limited sample size, the Student's t-distribution was adopted as the appropriate statistical model.

Table 8. Estimated tension properties

	ence: 99% ore: 2.728	М	SD	± Margin
F _{max'}	[N/thr]	4.916	0.205	0.095
R_{p02}	[MPa]	60.047	4.228	1.950
R _m	[MPa]	63.065	2.695	1.243
Ε	[MPa]	2531	390.505	180.094
\mathcal{E}_{p02}	[-]	0.026	0.004	0.002
\mathcal{E}_m	[-]	0.028	0.003	0.002

The experimental results indicate that a single PLA 3D-printed filament can sustain a maximum tensile force of 4.916 ± 0.095 N with 99% statistical confidence. The stress-strain behavior does not exhibit a distinct yield point separating elastic and plastic deformation. However, the specimens demonstrate consistent values for 0.2% offset yield strength (R_{p02}) , Young's modulus, and elongation at break, suggesting reproducible mechanical performance under tensile loading.

4. CONCLUSION

This research offers a focused tribute to the tensile characteristics of PLA filament, specifically in the form of isolated, printed threads, an aspect often overlooked in broader additive manufacturing research. By steering away from traditional bulk specimens and instead targeting individual thread lines, the study honors the material's micro-scale structural behavior and its contribution to the macro-scale integrity of printed components.

The testing approach was designed not only to evaluate mechanical parameters, such as ultimate tensile strength, elongation, and modulus, but also to highlight the crucial influence of thread survival throughout deformation. Observations reveal that the mechanical reliability of a PLA structure under tensile load is deeply tied to the ability of its embedded threads to remain unbroken up to the point of maximum strength. This insight emphasizes that preserving the continuity and cohesion of as many threads as possible during stress application is not just beneficial, it is essential for ensuring optimal performance in thin-walled or thread-reliant structures.

The experimental results revealed slightly lower overall tensile properties than anticipated for the specified filament manufacturer. While within acceptable variation ranges, this deviation suggests that material performance may be influenced by factors beyond standard specifications, such as batch consistency, thermal history during printing, or subtle variations in filament composition. Further work is should determine

whether these findings are systematic or anomalous, and to assess their impact on the mechanical properties.

Overall, the results lay the groundwork for refining FDM printing strategies aimed at thread-based optimization, offering meaningful implications for adaptive design and high-precision manufacturing where material efficiency and structural dependability converge.

ACKNOWLEDGEMENT

This research was financially supported by the Ministry of Science, Technological Development and Innovation of the Republic of Serbia (Contract No. 451-03-137/2025-03/200109).

REFERENCES

- [1] ASTM D638-14 Standard Test Method for Tensile Properties of Plastics, 2022.
- [2] ISO 527-1:2019 Plastics Determination of tensile properties. Part 1: General principles, 2019.
- [3] Yeole, Shivraj Narayan: Tensile Testing and Evaluation of 3D Printed PLA Specimens as per ASTM D638 Type-IV Standard, In book: Innovative Design, Analysis and Development Practices in Aerospace and Automotive Engineering (I-DAD 2018), pp.79-95, 2018.
- [4] B. Salvatore, R. Torre. Tensile and Compressive Behavior in the Experimental Tests for PLA Specimens Produced via Fused Deposition Modelling Technique, Journal of Composites Science 4, no. 3: 140, 2020.
- [5] Poddar, M. K., & Sarangi, S. K. An experimental analysis of poly-lactic acid (PLA) filament manufacturing for the 3D printer using Taguchi and analysis of variance (ANOVA). SSRG International Journal of Mechanical Engineering, 11(3), 1–10, 2024.
- [6] Domerg, M., Ostre, B., Belec, L., Berlioz, S., Joliff, Y., & Grunevald, Y. H. Aging effects at room temperature and process parameters on 3Dprinted PLA tensile properties. Progress in Additive Manufacturing, 9, 2427–2443, 2024.

- [7] Stojković, J.R., Turudija, R. A Review of 3D Printed Carbon Fiber Reinforced PLA Composites in Fused Filament Fabrication. Innovative Mechanical Engineering, Vol. 1, No. 2, pp. 58–79, 2022.
- [8] Alparslan, C., Bayraktar, Ş., & Gupta, K. A comparative study on mechanical performance of PLA, ABS, and CF materials fabricated by fused deposition modeling. Facta Universitatis, Series: Mechanical Engineering, 22(1), 1–12, 2024.
- [9] https://www.crealitycloud.com, accessed: 07/22/2025.
- [10] ISO 527-3:2018 Plastics Determination of tensile properties Part 3: Test conditions for films and sheets, 2018.
- [11] ISO 7500-1:2018 Metallic materials Calibration and verification of static uniaxial testing machines Part 1: Tension/compression testing machines Calibration and verification of the force-measuring system, 2023.
- [12] SRPS EN ISO 9513:2014 Metallic materials Calibration of extensometer systems used in uniaxial testing (ISO 9513:2012, Corrected version 2015-06), 2014.